Spectrochimica Acta Part A: Molecular and Biomolecular Spectroscopy 284 (2023) 121819

Contents lists available at ScienceDirect

Spectrochimica Acta Part A: Molecular and Biomolecular Spectroscopy

journal homepage: www.journals.elsevier.com/spectrochimica-acta-part-a-molecular-and-biomolecular-spectroscopy

Secondary structure alterations of RBC assessed by FTIR-ATR in correlation to 2,3-DPG levels in ApoE/LDLR$^{-/-}$ Mice

Fatih Celal Alcicek [a], Aneta Blat [a,b], Wiktoria Rutkowska [a,b], Katarzyna Bulat [a,c], Ewa Szczesny-Malysiak [a], Magdalena Franczyk-Zarow [d], Renata Kostogrys [d], Jakub Dybas [a,*], Katarzyna M. Marzec [a,c,*]

[a] Jagiellonian Centre for Experimental Therapeutics, Jagiellonian University, 14 Bobrzynskiego St., 30-348 Krakow, Poland
[b] Faculty of Chemistry, Jagiellonian University, 2 Gronostajowa St., 30-387 Krakow, Poland
[c] Łukasiewicz Research Network, Krakow Institute of Technology, 73 Zakopianska St., 30-418 Krakow, Poland
[d] Department of Human Nutrition and Dietetics, Faculty of Food Technology, University of Agriculture, 122 Balicka St., 30–149 Krakow, Poland

HIGHLIGHTS

- Sex, age, and disease progression have an impact on red blood cells (RBCs);
- Sex-related differences are prominent in older ApoE/LDLR$^{-/-}$ mice;
- Female RBCs are less prone to the alterations with progression of atherosclerosis;
- 2,3-DPG levels in RBCs show link to the hemoglobin secondary structure alterations.

GRAPHICAL ABSTRACT

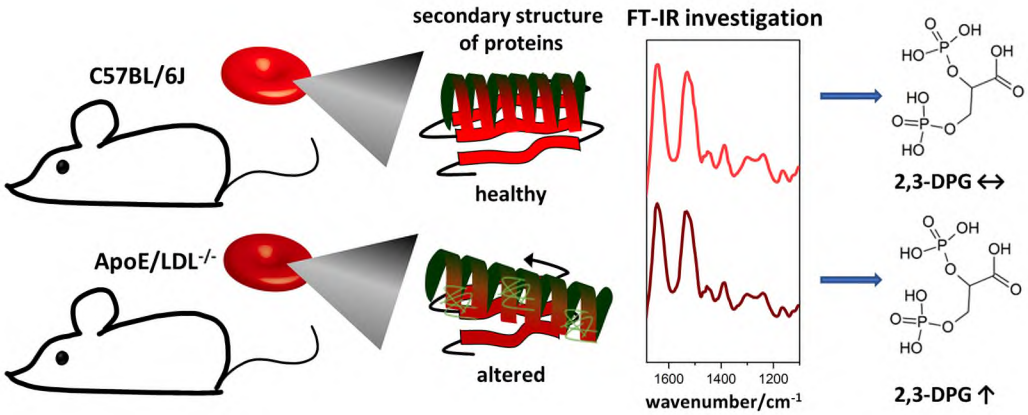

ARTICLE INFO

Keywords:
Red blood cells
Haemoglobin, 2,3-DPG
Fourier transform infrared spectroscopy

ABSTRACT

In the present study, we characterized the secondary structure alterations of intact red blood cells (RBCs) cytosol with special attention to the sex-related alterations in 8- and 24-week-old female and male ApoE/LDLR$^{-/-}$ mice, compared to age-matched female and male C57BL/6J control animals. Results were obtained with previously established methodology based on Fourier transform infrared spectroscopy-attenuated total reflectance (FTIR-ATR). Additionally, we evaluated 2,3-DPG levels in the RBCs and showed its potential link to the hemoglobin (Hb) secondary structure alterations. Considering Hb structure alterations probed by FTIR-ATR, the ratio of turns to α–helices in 8-week-old ApoE/LDLR$^{-/-}$ mice suggested more pronounced secondary structure alterations within the RBCs than in the age-matched control. Sex-related differences were observed solely in 24-week-old male ApoE/LDLR$^{-/-}$ mice, which showed statistically significant increase in the secondary structure alterations

* Corresponding authors at: Jagiellonian Centre for Experimental Therapeutics, Jagiellonian University, 14 Bobrzynskiego St., 30-348 Krakow, Poland (K.M. Marzec, J. Dybas) and Łukasiewicz Research Network, Krakow Institute of Technology, 73 Zakopianska St., 30-418 Krakow, Poland (K.M. Marzec).
E-mail addresses: jakub.dybas@uj.edu.pl (J. Dybas), katarzyna.marzec@kit.lukasiewicz.gov.pl (K.M. Marzec).

https://doi.org/10.1016/j.saa.2022.121819
Received 31 May 2022; Received in revised form 12 August 2022; Accepted 29 August 2022
Available online 3 September 2022

compared to 24-week-old female ApoE/LDLR$^{-/-}$ mice. Similar to the secondary structure alterations, no sex-related differences were observed in the levels of 2,3-DPG in RBCs, except for 24-week-old male ApoE/LDLR$^{-/-}$ mice, which showed significantly higher levels compared to the age-matched female ApoE/LDLR$^{-/-}$ mice. Considering the age-related alterations, we observed significant increases in the intracellular 2,3-DPG of RBCs with animals' age in all studied groups, except for female ApoE/LDLR$^{-/-}$ mice, where a significant difference was not reported. This suggests the clear correlation between secondary structure of Hb alterations and 2,3-DPG levels for male and female murine RBC and proves a higher resistance of older female RBCs to the secondary structure changes with progression of atherosclerosis. Moreover, it may be concluded that higher 2,3-DPG levels in RBCs occurred in response to the secondary structure alterations of Hb in ApoE/LDLR$^{-/-}$ mice.

1. Introduction

Red blood cells (RBCs) are exclusively differentiated to perform their key function – deliver oxygen to each cell within living organisms. This function is ensured by the substantial amount of hemoglobin (Hb) molecules constituting up to 95 % of the whole RBCs' protein content, as well as by the unique, flexible RBC membrane allowing them to pass through the tiniest capillaries [1–5]. Hemoglobin is a tetrameric protein, in which each of four globin subunits is bounded covalently with one heme molecule that serves as a prosthetic group [6]. Each heme comprises iron protoporphyrin IX, which is solely responsible for oxygen carrying and delivery. During the oxygenation process, oxygen molecules bind to one of four heme molecules within Hb, initiating changes in the Hb quaternary structure, what gradually increases Hb oxygen affinity and helps each subsequent oxygen molecule to bind more efficiently to the heme iron ion. This phenomenon is possible due to the relaxation of Hb subunits, and change of the Hb quaternary structure from T (tense, deoxygenated/deoxyHb) into R (relaxed, oxygenated/oxyHb) [7]. The process of oxygenation is controlled allosterically, what is possible due to the structural shape changes of Hb induced by several factors, e.g., intracellular level of 2,3-diphosphoglycerate (2,3-DPG) that regulates the affinity of Hb for oxygen [8,9]. Higher 2,3-DPG concentration leads to a decrease in Hb oxygen affinity, and vice versa. Additionally, RBC alterations result in changes in the secondary structure of Hb which may have an impact on the quaternary structure that affects the oxygen affinity of Hb [10,11].

Previously, we have demonstrated that the label-free vibrational spectroscopy techniques, including Fourier transform infrared spectroscopy-attenuated total reflectance (FTIR-ATR), can be successfully applied to determine the biochemical composition of isolated RBC membranes and intact RBCs in a semi-quantitative way, respectively [10,12–14]. Because the protein content of RBC cytosol is dominated by Hb molecules, therefore, application of FTIR-ATR spectroscopy on intact RBCs is much more suitable in comparison to Raman Spectroscopy (RS), where spectra are overlapped by strong resonant signal from heme [15]. FTIR-ATR could reveal insight into alterations of the secondary structure of RBC cytosol proteins, which henceforth will be referred to as only Hb proteins, since it comprises the vast majority of the total protein content in RBCs. Such alterations in the secondary structure of Hb protein may affect its functional quaternary structure. Importantly, Hb is primarily an α–helical protein and every change in its composition suggests RBC alterations [16].

In our previous work, we have already analyzed age- and atherosclerosis-related erythropathies in ApoE/LDLR$^{-/-}$ mice [11]. However, in that paper we focused on the analysis of RBCs isolated only from male mice. Our recent findings which clearly showed sex-specific differences in ATP levels, as well as various other important parameters of RBCs isolated from ApoE/LDLR$^{-/-}$ mice [17], suggested continuation of research towards attempting an additional analysis of the changes in the secondary structure of Hb proteins in RBCs in relation to mice sex. We have already reported that there is a strict relation between progressive alterations in secondary structures of Hb and the age of stored human RBCs [10], namely, formation of β-sheets, decrease in α-helices, and increase in intramolecular hydrogen bonding formation. In case of male murine RBCs, we have defined the age-related alterations that include a decrease in the ratio of turns to α-helices, as well as the atherosclerosis-related alterations that include an increase in the ratio of unordered conformations to α-helices. However, we have only mentioned that classical regulation by 2,3-DPG should also be taken into consideration in this type of study. As it is known that 2,3-DPG content allosterically regulates the oxygen affinity of Hb [8,9], in this work we have extended the analysis of RBC secondary structure by additional analysis of statistically significant number of male as well as female murine RBCs in correlation to their 2,3-DPG levels.

2. Methods and materials

2.1. Animal models and blood collection

Murine model of atherosclerosis (8- and 24-week-old, female and male, N = 6–10), ApoE/LDLR$^{-/-}$ [18], bred at University of Agriculture in Krakow, and matched wild-type controls (8- and 24-week-old, female and male, N = 6–8), C57BL/6J, bred at the Jackson Lab (Bar Harbor, Maine, USA), were used for the experiments. Mice were housed at the animal facility of Jagiellonian Centre for Experimental Therapeutics, Jagiellonian University in Krakow, in the conditions of 12-hour light/dark cycle, standard rodent chow diet and unlimited access to drinking water. All animal procedures were in accordance with the Guide for the Care and Use of Laboratory Animals published by the US National Institutes of Health (NIH Publication No. 85–23, revised 1985) as well as with the local Ethical Committee on Animal Experiments in Krakow. The number of mice in each given experimental group is stated in the captions of the corresponding figures.

Mice were anesthetized via intraperitoneal injection of overdose ketamine (100 mg/kg) and xylazine (10 mg/kg) mixture before sacrifice. Whole blood samples were collected directly from the right ventricle with a syringe containing heparin as an anticoagulant (10 units/mL).

2.2. RBC isolation

After blood collection, a complete blood count was performed. Whole blood samples were subjected to centrifugation (acceleration: 500 × g, run time: 10 min, 4 °C, soft stop) up to 1 h after collection. The plasma and buffy coat were aspirated after centrifugation. RBCs were washed with the daily buffer solution (DBS). Subsequently, centrifugation was repeated 2 times. Each time, DBS was added for rinsing before centrifugation and supernatant was aspirated. The DBS was prepared on the same day for each experiment, and it contained: 21.0 mM Tris Base, 140.5 mM NaCl, 4.7 mM KCl, 2.0 mM $CaCl_2$, 1.2 mM $MgSO_4$, 5.5 mM glucose and 76 μM bovine serum albumin, with a final pH adjusted to 7.40. All chemicals were dissolved in distilled water and the solution was filtered through a pleated filter with 0.22 μm pore size.

2.3. FTIR-ATR measurements with data analysis and processing

FTIR measurements were performed to characterize the changes in the secondary structure of Hb in RBCs. Briefly, FTIR spectra were

collected for the pure fraction of isolated RBCs using a Bruker Alpha FTIR spectrometer equipped with a single-bounce diamond ATR crystal. Spectra were acquired with a 4 cm^{-1} spectral resolution in the range of 3800–900 cm^{-1} by co-adding 64 scans. The smears of isolated RBCs were prepared by deposition of 5 μL of each sample on the CaF_2 windows and air drying in ambient conditions for approximately 1 h. Each spectrum was recorded for approximately 2 min. The background of the clean ATR crystal was recorded before each measurement. Five replicates for each sample were collected. Each sample of isolated RBCs was prepared and placed on CaF_2 slides in the exact same way. Therefore,

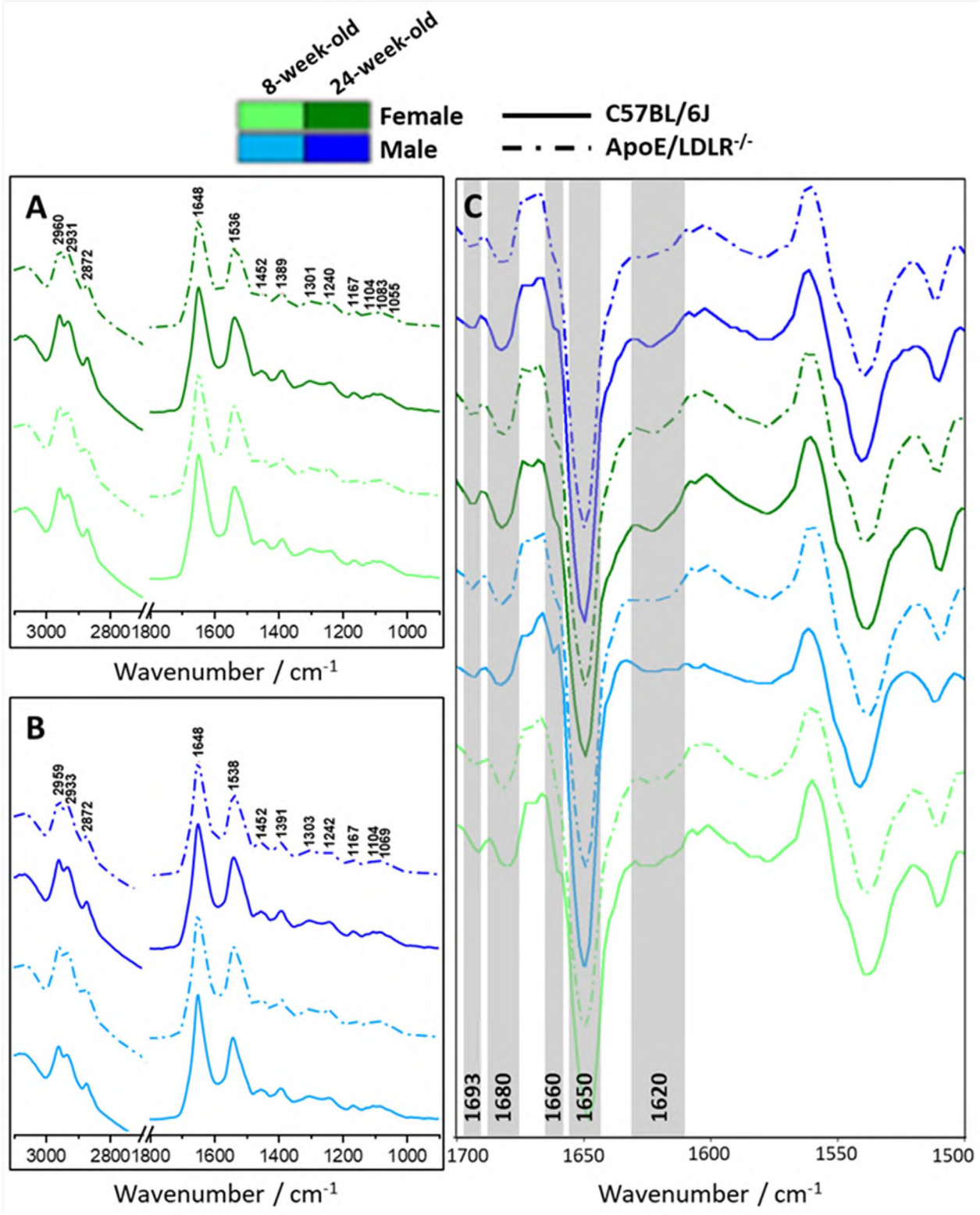

Fig. 1. Average FTIR-ATR spectra of unfixed intact RBCs isolated from female (A) and male (B), 8- (light blue and light green) and 24-week-old (dark green and dark blue), C57BL/6J (solid line, N = 6 – 10) and ApoE/$LDLR^{-/-}$ (dash and dot line, N = 6 – 8) mice. Second derivatives of averaged FTIR-ATR spectra (C) displayed in the 1700–1500 cm^{-1} spectral regions.

eventual impact of DBS solution residues on comparative analysis can be neglected.

To determine the integral intensity of the selected bands, the second derivatives of IR spectra were calculated using a Savitzky-Golay method with nine smoothing points and vector normalized in the "fingerprint region" (900–1800 cm^{-1}). Next, the areas above the peaks were calculated using OPUS 7.2 software (Bruker Optics, Billerica, Massachusetts, USA).

Box charts of the bands' ratios were constructed using OriginPro 2020b software (OriginLab, Northampton, Massachusetts, USA). Statistics were calculated according to the results of normality assessment performed using Shapiro–Wilk test. The data did not meet normality requirement; therefore, the Mann-Whitney test was performed, and results were shown as box diagrams containing mean, median, and interquartile range together with min–max whiskers.

2.4. Determination of intracellular 2,3-DPG levels and data analysis

Intracellular 2,3-DPG levels were measured using a commercially available ELISA kit on RBCs subjected to subsequent hemolysis (Abbexa ltd, Cambridge, UK) according to the manufacturer's instructions. This kit is based on competitive enzyme-linked immuno-sorbent assay technology. An antibody is pre-coated onto a 96-well plate. Standards, test samples, and biotin-conjugated reagent were all added to the wells and incubated. A competitive inhibition reaction took place between the biotin-labelled 2,3-DPG and the unlabeled-2,3-DPG on the pre-coated antibody. The horseradish peroxidase (HRP)-conjugated reagent was then added, and the whole plate was incubated. Unbound conjugates were removed using a wash buffer at each stage. TMB (3,3′,5,5′-Tetramethylbenzidine) substrate was used to quantify the HRP enzymatic reaction. After TMB substrate was added, only wells that contained sufficient 2,3-DPG would produce a blue colored product, which then changes to yellow after addition of the acidic stop solution. The intensity of yellow color was inversely proportional to the 2,3-DPG amount bound on the plate. The OD was measured spectrophotometrically at 450 nm in a microplate reader, from which the concentration of 2,3-DPG was calculated.

The data sets were analyzed in OriginPro 2020b (OriginLab, Northampton, Massachusetts, USA) software. Normality was assessed using Shapiro-Wilk test. The data are expressed as bar plots (mean ± SE) and the significance was calculated using one-way ANOVA with Tukey's test.

3. Results and discussion

3.1. Alterations in the secondary structure of intact murine RBCs

FTIR-ATR Spectroscopy was performed to investigate alterations in the secondary structure of cytosol proteins in intact RBCs isolated from female and male, 8- and 24-week-old, C57BL/6J and ApoE/LDLR$^{-/-}$ mice. The average FTIR-ATR spectra of intact RBCs in female and male mice were displayed in Fig. 1**A and B**, respectively. In Fig. 1**C**, the second derivatives of averaged FTIR-ATR spectra in the 1700–1500 cm^{-1} spectral range were presented. They revealed the changes of intensities for some components of amide I band corresponding to the different secondary structures of cytosol proteins, in particular Hb [19,20].

Herein, we evaluated sex-, disease-, and age-related alterations in the secondary structure of Hb molecules by calculating the ratios of turns, intramolecular aggregates, and intermolecular aggregates to α–helices. The presence of intermolecular aggregates can be evidenced by simultaneous occurrence of two characteristic components at 1620 and 1693 on the obtained FTIR spectra. We calculated the integral intensities of chosen marker bands (ca. 1650, 1660, 1680, and 1693 cm^{-1}, which indicate the presence of following structures: α-helices, turns, intramolecular aggregates, and intermolecular aggregates, respectively) in a semi-quantitative manner for intact RBCs from the second derivative of averaged FTIR-ATR spectra and demonstrated in Fig. 2 as ratios, 1660/1650 (Fig. 2**A**), 1680/1650 (Fig. 2**B**), and 1693/1650 (Fig. 2**C**). Band assignments and integration ranges were summarized in Table 1.

Turns favor the formation of the globular shape of the Hb subunits by the reversing the direction of the polypeptide chain composed of α-helices [24]. We observed lower mean values in turns to α-helices ratio in ApoE/LDLR$^{-/-}$ mice compared to age-matched controls for both female and male mice (Fig. 2**A**) what suggests loosening of the Hb structure. However, the observed decreases were statistically significant only for 8-week-old females and males. This clearly proves that the RBCs isolated from young mice displayed significant alterations in the secondary structure of Hb proteins compared to their age matched control. Furthermore, such findings were consistent with our previous results obtained solely for males, where we reported the biggest changes of the secondary structure in the RBCs isolated from 5-week-old ApoE/LDLR$^{-/-}$ mice with hypercholesterolemia [11]. Interestingly, no significant difference in the ratio of turns to α-helices was observed between males and females in 8-week-old C57BL/6J and ApoE/LDLR$^{-/-}$ mice. On the other hand, older animals showed sex-related difference in the ratio of turns to α-helices. Yet solely 24-week-old ApoE/LDLR$^{-/-}$ male mice showed a statistically significant increase in the secondary structure alterations of RBC cytosol proteins compared to female 24-week-old ApoE/LDLR$^{-/-}$ mice. This suggests a higher resistance of female RBCs to the secondary structure changes connected with progression of atherosclerosis in older animals.

An addition to the alterations in the ratio of turns to α–helices, we were able to characterize intramolecular and intermolecular aggregates to α–helices ratios, revealed by integrating the second derivatives of FTIR-ATR spectra. The ratio of intramolecular aggregates to α-helices (Fig. 2**B**), expressed by the 1680/1650 cm^{-1} ratio, displayed downward trends in female and male ApoE/LDLR$^{-/-}$ mice compared to the age-matched controls. This observation may suggest unfolding of proteins (weakening of intramolecular interactions) which can lead to their aggregation due to the greater propensity of unfolded chains to form non-random aggregates [10,25]. The decreases in intramolecular aggregates to α–helices ratios were statistically significant for both female and male ApoE/LDLR$^{-/-}$ mice in comparison to the suitable control groups. We observed no sex-related differences in any of studied groups except for the meaningfully lower values of ratios for 24-week-old male ApoE/LDLR$^{-/-}$ in relation to age-matched female ApoE/LDLR$^{-/-}$. Interestingly, this observation was compatible with results obtained for turns to α-helices ratio (Fig. 2**A**) proving the higher sensibility of male RBCs to the secondary structure changes of proteins caused by the atherosclerosis in older mice. Male and female C57BL/6J mice showed significant decreases in the ratio of intramolecular aggregates to α-helices with age.

On the other hand, the ratio of intermolecular aggregates (aggregation-specific β-sheets) to α-helices (Fig. 2**C**), expressed by the 1693/1650 cm^{-1} ratio [21–23], was significantly increased in female and male ApoE/LDLR$^{-/-}$ mice compared to the age-matched controls. Such finding could indicate aggregation process of proteins occurring as a result of the exposure of C═O and N—H groups of proteins, leading to hydrogen bonds formation between polypeptide chains in neighbouring protein molecules. Interestingly, 8-week-old male control and ApoE/LDLR$^{-/-}$ mice displayed significantly lower intermolecular aggregates to α–helices ratio compared to their age-matched females; however, no difference was observed between 24-week-old female and male mice. Moreover, no age-related differences were observed in the ratio of intermolecular aggregates to α–helices in female control and ApoE/LDLR$^{-/-}$ mice in contrary to male mice, which displayed significant increase in the ratio with age progress, suggesting higher resistance against age-related alterations in females. Unfortunately, we were not able to analyze changes in the content of unordered structures as in our previous work, due to the low intensity of the 1640 cm^{-1} band in the obtained spectra.

Based on the obtained results, it may be suggested that peptide chains in Hb partially unfold due to processes connected with

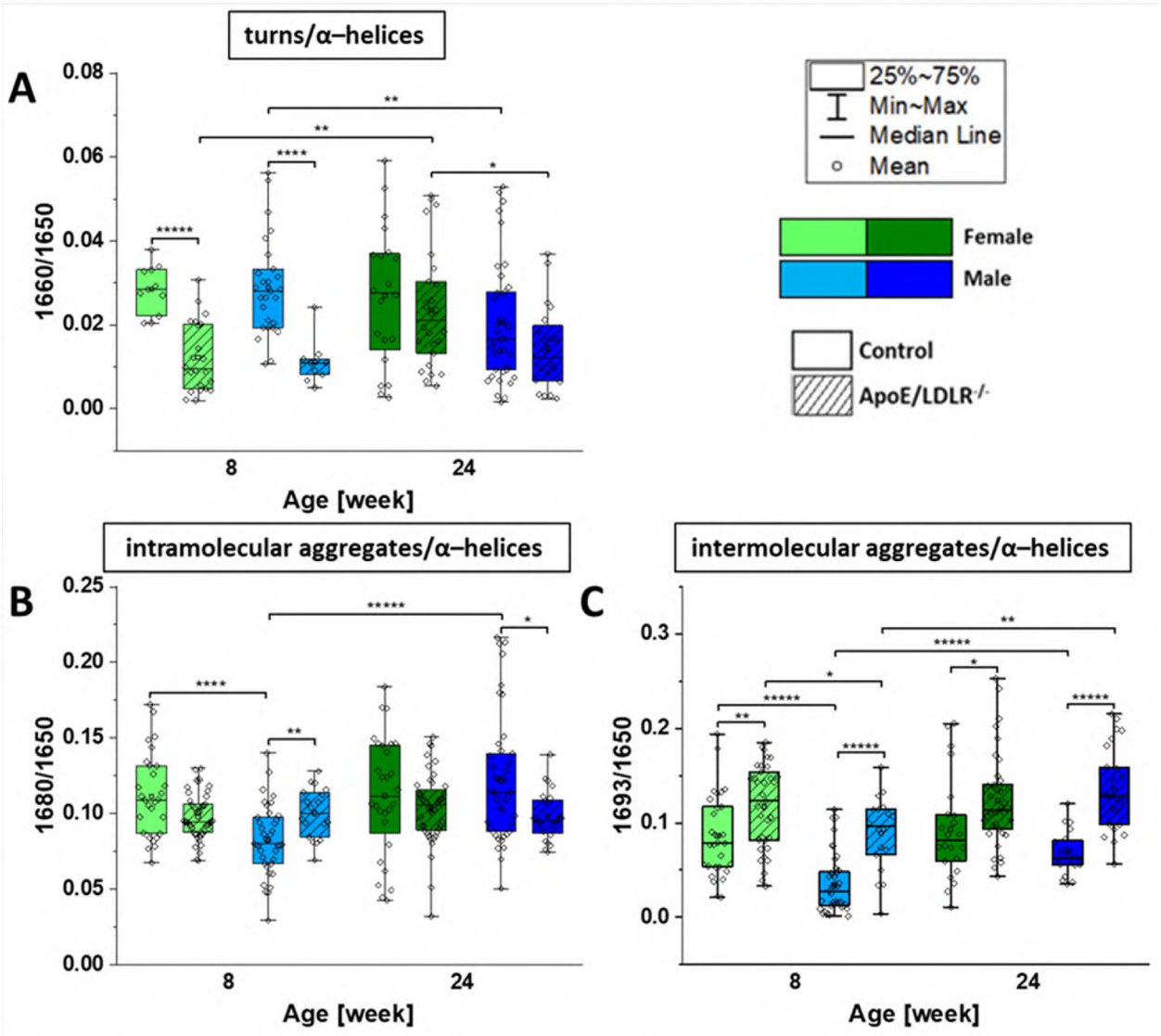

Fig. 2. Ratios calculated for the integral intensities of absorption bands in the FTIR-ATR spectra at 1660/1650 cm^{-1} (A), 1680/1650 cm^{-1} (B), and 1693/1650 cm^{-1} (C) showing alterations in secondary structures of proteins in cytosol of RBCs isolated from female and male, 8- and 24-week-old, C57BL/6J (N = 6 – 10) and ApoE/LDLR$^{-/-}$ (N = 6 – 8) mice, i.e., turns to α–helices, intramolecular aggregates to α–helices, and intermolecular aggregates to α–helices, respectively. The integration regions and band assignments are depicted in Table 1. Normality was assessed using Shapiro-Wilk test. The data are expressed as box plots (median and interquartile range min–max whiskers) and the significance was calculated with Mann–Whitney test (*$P < 0.05$, **$P < 0.01$, ****$P < 10^{-4}$, *****$P < 10^{-5}$).

Table 1
Definition of the assignment and shorthand notation of the main FTIR-ATR spectroscopic markers for which the integral intensities were applied.

	Band wavenumber (Integration ranges)	**Band assignment** [19–23]	
FTIR-ATR bands	1693 cm^{-1} (1702–1690)	intermolecular aggregates	Amide I C=O stretching and N—H deformation
FTIR-ATR bands	1680 cm^{-1} (1689–1675)	intramolecular aggregates	
	1660 cm^{-1} (1666–1660)	turns	
	1650 cm^{-1} (1660–1634)	α-helices	

progression of atherosclerosis and aging. It might be facilitated by the simultaneous appearance of two changes connected with the protein secondary structure: decrease in turns and weakening of the intramolecular interactions. Moreover, displayed increased intermolecular aggregates in ApoE/LDLR$^{-/-}$ mice and aged male mice are most likely resulted from the weakened intramolecular interactions. The effect of this process was more pronounced for the RBCs in atherosclerotic mice. Sex-related differences appeared in the older ApoE/LDLR$^{-/-}$ mice for turns but in the younger control and ApoE/LDLR$^{-/-}$ mice for the intermolecular aggregates, and again suggested higher resistance of female RBCs to Hb structure alterations. Additional comparison of the data was provided by principal component analysis (PCA) included in the supplementary materials (Figure SM1). The results of carried out PCA stayed in agreement with the trends of the observed alterations according to analysis of the PC2 loadings, however, the clear discrimination between groups was not possible due to the subtle changes of the spectral profiles between studied groups.

3.2. Intracellular 2,3-DPG levels of murine RBCs

2,3-DPG is present in RBCs as an intermediary metabolite of the Embden-Meyerhof glycolytic pathway, the main pathway for ATP production in RBCs [26]. 2,3-DPG levels in RBCs and the affinity of Hb to

oxygen molecules exhibit an inverse correlation [8,9]. In our study, intracellular 2,3-DPG levels of RBCs (Fig. 3) isolated from both female and male ApoE/LDLR$^{-/-}$ mice were always higher compared to age-matched controls, yet the only significant difference was observed in 24-week-old males, what suggests lower Hb affinity to oxygen molecules in ApoE/LDLR$^{-/-}$ mice.

Hypercholesterolemia results in an increase in the cholesterol content in RBC membranes, which reduces oxygen diffusion through the membrane [27]. Due to this effect, previously we have suggested that hypercholesterolemia in ApoE/LDLR$^{-/-}$ mice could cause higher Hb levels in RBCs compared to age-matched controls, in order to increase the oxygenation of tissues [17]. Yet, we observed higher 2,3-DPG levels per Hb (~1.2–1.8 times) in RBCs acquired from ApoE/LDLR$^{-/-}$ mice compared to the age-matched controls in all studied groups, what indicates that the increase in 2,3-DPG levels was higher than the increase in Hb levels. Higher 2,3-DPG levels result in lower oxygen affinity of Hb [8,9]. Collectively, we may speculate that because of the higher cholesterol content in RBC membrane and related hindering of the oxygen diffusion, higher 2,3-DPG levels of RBCs in ApoE/LDLR$^{-/-}$ mice may serve as a compensation mechanism, facilitating oxygen release to the tissues. Nevertheless, further studies are required.

RBCs acquired from female 8-week-old C57BL/6J and ApoE/LDLR$^{-/-}$ mice showed upward trend in intracellular 2,3-DPG levels compared to age-matched male mice. However, 24-week-old female ApoE/LDLR$^{-/-}$ mice showed significantly lower levels of 2,3-DPG in their RBCs compared to age-matched male mice, while C57BL/6J mice showed lack of sex-related difference. Such findings may indicate slightly higher oxygen affinity of Hb molecules in murine RBCs of young males, both control and ApoE/LDLR$^{-/-}$ than females, while an opposite stance is seen in older mice. Furthermore, we observed significant increases in the level of 2,3-DPG in RBCs with aging for all studied groups, except for female ApoE/LDLR$^{-/-}$ mice, where the reported increase was not significant.

Collectively, there were no sex-related differences in the levels of 2,3-DPG in RBCs (similar observation was found for human RBCs [28]), except for 24-week-old male ApoE/LDLR$^{-/-}$ mice, which showed significantly higher levels compared to age-matched female ApoE/LDLR$^{-/-}$ mice. Importantly, it must be pointed out, that significant change between female and male 24-week-old ApoE/LDLR$^{-/-}$ mice, could be related with differences in amount of Hb between those groups. However, in contrast to human studies, where 2,3-DPG levels in RBCs decreased with age [28], our findings showed that 2,3-DPG levels in RBCs significantly increased with age in all studied mice groups, except for female ApoE/LDLR$^{-/-}$ mice, where an increase occurred as well, but was not significant. Accordingly, one can suggest that Hb affinity to oxygen molecules decreases with the age progression in murine RBCs, since 2,3-DPG level in RBCs is one the major modulators of Hb affinity to oxygen [8,9].

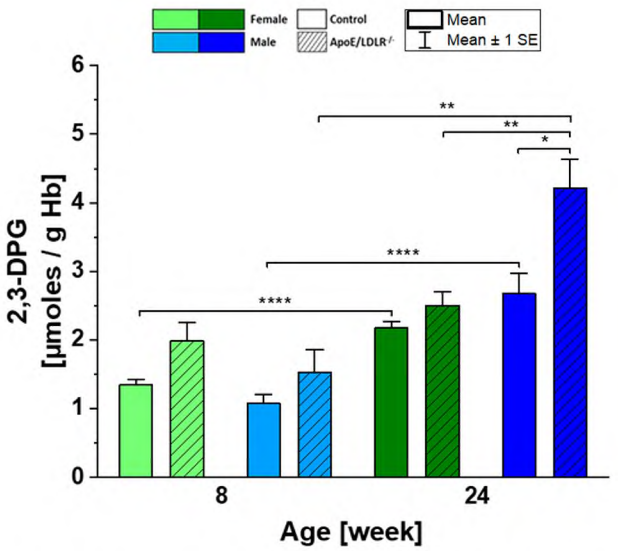

Fig. 3. 2,3-Diphosphoglycerate (2,3-DPG) levels in red blood cells isolated from female and male, 8- and 24-week-old C57BL/6J (N = 4 – 9) and ApoE/LDLR$^{-/-}$ (N = 4 – 13) mice. Normality was assessed using Shapiro-Wilk test. The data are expressed as bar plots (mean ± SE) and the significance was calculated using one-way ANOVA with Tukey's test (*P < 0.05, **P < 0.01, ****P < 10^{-4}).

4. Conclusions

Previously, we have reported that irreversible alterations in the secondary structure of Hb increased progressively with the time of storage of human RBCs, and influenced the quaternary structure of Hb leading to the formation of the R' quaternary structure of Hb [10]. This had an impact on oxygen uptake and release leading to their artificial increase. We have reported that the higher the level of secondary and quaternary structures alteration of Hb, the higher is the level of oxyHb within RBCs [10]. Additionally, we have previously reported higher oxygen carrying capacity of RBCs in male ApoE/LDLR$^{-/-}$ mice compared to the age-matched controls [11], which was defined as a result of the alterations in the secondary structure of Hb proteins. Our previous results clearly proved that secondary structure alterations of Hb, which lead to changes in the quaternary structure of Hb, in consequence lead to a shift in its oxygen affinity.

In the present study, we found that RBCs isolated from ApoE/LDLR$^{-/-}$ mice exhibited notable changes in the secondary structure of Hb comparing to their age-matched controls. Moreover, sex-related changes were observed in only for intramolecular aggregates to α–helices ratio, in RBCs isolated from young control and ApoE/LDLR$^{-/-}$ mice. However, older mice groups exhibited sex-related differences in other secondary structure alterations, i.e., 24-week-old male ApoE/LDLR$^{-/-}$ mice displayed a statistically significant increase in the ratio of turns to α–helices compared to 24-week-old female ApoE/LDLR$^{-/-}$ mice. These indicated a higher resistance of female RBCs to secondary structure changes due to atherosclerosis in case of older animals. Such trend stays in correlation with the levels of 2,3-DPG, where no sex-related differences were observed for young murine RBCs of both control and ApoE/LDLR$^{-/-}$ mice. Moreover, similar as for the secondary structure alterations of Hb, sex-related changes were identified in 24-week-old male ApoE/LDLR$^{-/-}$ mice, which showed significantly higher levels compared to age-matched female ApoE/LDLR$^{-/-}$ mice. This suggests a clear-cut correlation between the alterations in the secondary structure of Hb and 2,3-DPG levels in RBCs for male and female mice groups (in both control and ApoE/LDLR$^{-/-}$ mice). The higher the 2,3-DPG level within the RBC, the higher the secondary structure alterations of their cytosol proteins and vice versa.

Ordinarily, 2,3-DPG binds to deoxyHb and stabilizes the T state, which results in lower Hb affinity to oxygen [9]. Consistently, lower 2,3-DPG levels are expected in RBCs isolated from ApoE/LDLR$^{-/-}$ mice, according to the reported higher oxygen carrying capacity of their RBCs [11]. However, our findings indicate contrarily. Namely, RBCs in ApoE/LDLR$^{-/-}$ mice exhibited higher oxygen carrying capacity despite their higher 2,3-DPG levels. Accordingly, we may speculate that the revealed alterations in the secondary structure of Hb protein in ApoE/LDLR$^{-/-}$ mice could be irreversible, as in stored human packed RBCs [10], which may lead to the higher oxygen carrying capacity. Accordingly, 2,3-DPG levels in RBCs were increased as a compensation mechanism in response to such irreversible alterations.

CRediT authorship contribution statement

Fatih Celal Alcicek: Conceptualization, Methodology, Validation, Investigation, Formal analysis, Visualization, Data curation, Writing – original draft. **Aneta Blat:** Methodology, Investigation, Formal analysis,

Visualization, Writing – review & editing. **Wiktoria Rutkowska:** Investigation, Formal analysis, Visualization, Writing – review & editing. **Katarzyna Bulat:** Investigation, Formal analysis, Writing – review & editing. **Ewa Szczesny-Malysiak:** Investigation, Formal analysis, Writing – review & editing. **Magdalena Franczyk-Zarow:** Resources. **Renata Kostogrys:** Resources. **Jakub Dybas:** Methodology, Validation, Investigation, Formal analysis, Visualization, Writing – review & editing. **Katarzyna M. Marzec:** Conceptualization, Methodology, Writing – review & editing, Project administration, Supervision, Funding acquisition.

Declaration of Competing Interest

The authors declare that they have no known competing financial interests or personal relationships that could have appeared to influence the work reported in this paper.

Data availability

Data will be made available on request.

Acknowledgments

This research was funded by the Polish National Science Centre, No. UMO- 2020/38/E/ST4/00197.

References

[1] K. Kaushansky, M.A. Lichtman, J.T. Prchal, et al., Hematology, 9th ed., McGraw-Hill Education, New York, 2016.
[2] J. Dybas, M.J. Bokamper, K.M. Marzec, P.J. Mak, Probing the structure-function relationship of hemoglobin in living human red blood cells, Spectrochim Acta - Part A Mol. Biomol. Spectrosc. 239 (2020), 118530.
[3] S.M. Hattangadi, P. Wong, L. Zhang, J. Flygare, H.F. Lodish, From stem cell to red cell: Regulation of erythropoiesis at multiple levels by multiple proteins, RNAs, and chromatin modifications, Blood 118 (24) (2011) 6258–6268.
[4] D. Melo, S. Rocha, S. Coimbra, S.A. Santos Interplay between Erythrocyte Peroxidases and Membrane. In: Erythrocyte. IntechOpen, 2019 doi:10.5772/intechopen.83590.
[5] R. Huisjes, A. Bogdanova, W.W. van Solinge, R.M. Schiffelers, L. Kaestner, R. van Wijk, Squeezing for life - Properties of red blood cell deformability, Front. Physiol. 9 (JUN) (2018) 656.
[6] D.A. Gell, Structure and function of haemoglobins, Blood Cells Mol. Dis. 70 (2018) 13–42.
[7] C. Thomas, A.B. Lumb, Physiology of haemoglobin, Contin Educ Anaesthesia, Crit Care Pain. 12 (5) (2012) 251–256.
[8] M.F. Perutz, Regulation of oxygen affinity of hemoglobin: Influence of structure of the globin on the heme iron, Annu. Rev. Biochem. 48 (1979) 327–386.
[9] R. Benesch, R.E. Benesch, The effect of organic phosphates from the human erythrocyte on the allosteric properties of hemoglobin, Biochem. Biophys. Res. Commun. 26 (2) (1967) 162–167.
[10] E. Szczesny-Malysiak, J. Dybas, A. Blat, et al., Irreversible alterations in the hemoglobin structure affect oxygen binding in human packed red blood cells, Biochim Biophys Acta - Mol Cell Res. 1867 (11) (2020), 118803.
[11] J. Dybas, K. Bulat, A. Blat, et al., Age–related and atherosclerosis–related erythropathy in ApoE/LDLR−/− mice, Biochim Biophys. Acta – Mol. Basis Dis. 1866 (12) (2020), 165972.
[12] J. Dybas, F.C. Alcicek, A. Wajda, et al., Trends in biomedical analysis of red blood cells – Raman spectroscopy against other spectroscopic, microscopic and classical techniques, TrAC - Trends Anal. Chem. 146 (2022), 116481.
[13] A. Blat, J. Dybas, M. Kaczmarska, et al., An analysis of isolated and intact rbc membranes - a comparison of a semiquantitative approach by means of FTIR, Nano-FTIR, and Raman Spectroscopies, Anal. Chem. 91 (15) (2019) 9867–9874.
[14] A. Blat, T. Stepanenko, K. Bulat, et al., Spectroscopic signature of red blood cells in a d-galactose-induced accelerated aging model, Int. J. Mol. Sci. 22 (5) (2021) 1–15.
[15] K.M. Marzec, D. Perez-Guaita, M. De Veij, et al., Red blood cells polarize green laser light revealing hemoglobin's enhanced non-fundamental Raman modes, ChemPhysChem 15 (18) (2014) 3963–3968.
[16] P. Prevelige, G.D. Fasman, Chou-Fasman Prediction of the Secondary Structure of Proteins. In: Prediction of Protein Structure and the Principles of Protein Conformation. Springer, Boston, MA, 1989, pp 391–416.
[17] F.C. Alcicek, T. Mohaissen, K. Bulat, et al., Sex-specific differences of adenosine triphosphate levels in red blood cells isolated from ApoE/LDLR double-deficient mice, Front. Physiol. 13 (2022) 223.
[18] S. Ishibashi, J. Herz, N. Maeda, J.L. Goldstein, M.S. Brown, The two-receptor model of lipoprotein clearance: Tests of the hypothesis in 'knockout' mice lacking the low density lipoprotein receptor, apolipoprotein E, or both proteins, Proc. Natl. Acad. Sci. U.S.A. 91 (10) (1994) 4431–4435.
[19] M. Mahato, P. Pal, T. Kamilya, R. Sarkar, A. Chaudhuri, G.B. Talapatra, Hemoglobin-silver interaction and bioconjugate formation: a spectroscopic study, J. Phys. Chem. B 114 (20) (2010) 7062–7070.
[20] A.K. Bhunia, T. Kamilya, S. Saha, Study of the adsorption of human hemoglobin to silver (Ag) nanoparticle surface for the detection of the unfolding of hemoglobin, Plasmonics 1 (2022) 1–18.
[21] P. Sassi, A. Giugliarelli, M. Paolantoni, A. Morresi, G. Onori, Unfolding and aggregation of lysozyme: a thermodynamic and kinetic study by FTIR spectroscopy, Biophys. Chem. 158 (1) (2011) 46–53.
[22] J. Milošević, R. Prodanović, N. Polović, On the protein fibrillation pathway: oligomer intermediates detection using ATR-FTIR spectroscopy, Molecules 26 (4) (2021), https://doi.org/10.3390/molecules26040970.
[23] N. Wilkosz, M. Czaja, S. Seweryn, et al., Molecular spectroscopic markers of abnormal protein aggregation, Molecules 25 (11) (2020) 2498.
[24] A.M.C. Marcelino, L.M. Gierasch, Roles of β-turns in protein folding: From peptide models to protein engineering, Biopolymers 89 (5) (2008) 380–391.
[25] K.E. Routledge, G.G. Tartaglia, G.W. Platt, M. Vendruscolo, S.E. Radford, Competition between Intramolecular and Intermolecular Interactions in an Amyloid-Forming Protein, J. Mol. Biol. 389 (4) (2009) 776–786.
[26] R. Van Wijk, W.W. Van Solinge, The energy-less red blood cell is lost: Erythrocyte enzyme abnormalities of glycolysis, Blood 106 (13) (2005) 4034–4042.
[27] H. Buchwald, T.J. O'Dea, H.J. Menchaca, V.N. Michalek, T.D. Rohde, Effect of plasma cholesterol on red blood cell oxygen transport, Clin. Exp. Pharmacol. Physiol. 27 (12) (2000) 951–955.
[28] Y. Purcell, B. Brozović, Red cell 2,3-diphosphoglycerate concentration in man decreases with age, Nature 251 (5475) (1974) 511–512.